Hypertension Research (2019) 42:329–340
https://doi.org/10.1038/s41440-018-0185-3

ARTICLE

The ATRQβ-001 vaccine improves cardiac function and prevents postinfarction cardiac remodeling in mice

Yajie Pan[1,2,3] · Zihua Zhou[1,2,3] · Hongrong Zhang[1,2,3] · Yanzhao Zhou[1,2,3] · Yingying Li[1,2,3] · Chang Li[1,2,3] · Xiao Chen[1,2,3] · Shijun Yang[1,2,3] · Yuhua Liao[1,2,3] · Zhihua Qiu[1,2,3]

Received: 28 June 2018 / Revised: 9 September 2018 / Accepted: 9 September 2018 / Published online: 26 December 2018

Abstract

We invented the ATRQβ-001 hypertension vaccine, which targeted angiotensin II type 1 receptor (AT_1R) and showed a desirable blocking effect for AT_1R. The purpose of this study was to investigate whether the ATRQβ-001 vaccine could improve cardiac function and prevent cardiac remodeling after acute myocardial infarction (AMI). C57BL/6 male mice were randomly assigned into four groups: sham + VLP, MI + VLP, MI + ATRQβ-001, and MI + valsartan. Mice were administered Qβ virus-like particle (Qβ-VLP, 100 μg/time), ATRQβ-001 vaccine (100 μg/time), and valsartan (6 mg/kg/day) before AMI, which was induced by permanently ligating the left anterior descending coronary artery. The effect of the ATRQβ-001 vaccine on cardiac function and cardiac remodeling was observed by following up for 1 week, 4 weeks, and 12 weeks post MI. The ATRQβ-001 vaccine significantly reduced sudden cardiac death and increased survival rates (compared with MI + VLP, 80% versus 55% and mean estimate (days) 68.4 ± 7.0 versus 47.8 ± 8.9, respectively; $p = 0.046$) post MI. Echocardiography showed that the ATRQβ-001 vaccine remarkably improved cardiac function (left ventricular ejection fraction, 24.8 ± 7.0% versus 13.2 ± 3.8%, $p = 0.005$) post MI. Histological analysis revealed that the ATRQβ-001 vaccine obviously mitigated myocardial inflammation, apoptosis, and fibrosis after AMI. Further, the ATRQβ-001 vaccine significantly inhibited the TGF-β1/Smad2/3 signaling pathway. Assessment of the renin-angiotensin system (RAS) demonstrated that the ATRQβ-001 vaccine did not cause obvious feedback of circulating RAS, but prominently attenuated the expression of AT_1R, compared with the other groups at 4 and 12 weeks after AMI. In conclusion, the ATRQβ-001 vaccine decreased mortality and improved cardiac function and remodeling after AMI.

Keywords ATRQβ-001 vaccine · Acute myocardial infarction · Cardiac remodeling · Angiotensin II receptor

Introduction

Acute myocardial infarction (AMI) involves a progression of deterioration toward heart failure, which leads to the irreversible impairment of heart function and is a major cause of mortality [1, 2]. Cardiac repair after AMI results from a complex series of events initiated by intense sterile inflammation and immune cell infiltration, followed by a reparative phase with resolution of inflammation, scar formation, and fibrosis in the following days [3, 4]. Activation of the renin–angiotensin system (RAS), through pro-inflammatory and pro-fibrotic effects, has been singled out as a key process in the left ventricular remodeling that occurs after AMI. In clinical treatment, RAS blockers, angiotensin-converting enzyme inhibitors and angiotensin II receptor blockers (ARBs) have proven to be efficacious in modulating the noxious environment and limiting left ventricular remodeling after AMI [5, 6].

These authors contributed equally: Yajie Pan, Zihua Zhou, and Hongrong Zhang

Supplementary information The online version of this article (https://doi.org/10.1038/s41440-018-0185-3) contains supplementary material, which is available to authorized users.

✉ Zhihua Qiu
qiu_zhihua512@163.com

1 Department of Cardiology, Union Hospital, Tongji Medical College, Huazhong University of Science and Technology, Wuhan 430022, China

2 Institute of Cardiology, Union Hospital, Tongji Medical College, Huazhong University of Science and Technology, Wuhan 430022, China

3 Key Lab of Molecular Biological Targeted Therapies of the Ministry of Education, Union Hospital, Tongji Medical College, Huazhong University of Science and Technology, Wuhan 430022, China

We previously invented a virus-like particle (VLP)-based antihypertensive vaccine against human and murine angiotensin II type 1 receptor (ATRQβ-001 vaccine), which could significantly reduce the blood pressure and protect target organs of hypertensive animals, as well as ameliorate atherosclerosis and nephropathy in animal models [7–9]. The half-life of the ATRQβ-001 vaccine antibody is far longer than ARBs presently used [7]. The ATRQβ-001 vaccine does not cause obvious feedback of RAS compared with ARBs [7–9]. Based on these findings, the ATRQβ-001 vaccine may play a role in preventing cardiac remodeling and have potential advantages relative to ARBs. To investigate the effect of the ATRQβ-001 vaccine on survival rate and cardiac function in different phases of AMI, this study spans three periods of 1 week, 4 weeks, and 12 weeks after AMI in mice. The results showed that the ATRQβ-001 vaccine obviously improved survival and cardiac function after AMI.

Materials and methods

Peptide synthesis and vaccine preparation

The ATR-001 peptide (amino-acid sequence, C-A-F-H-Y-E-S-Q) derived from the second extracellular loop of human AT_1R was synthesized by GL Ltd. (Shanghai, China). The purity was at least 98%. The ATR-001 peptide was covalently conjugated with Qβ virus-like particle (Qβ-VLP) by cross-linker Sulfo-SMCC (Thermo Scientific, USA) according to the manufacturer's instructions. The vaccine concentration was determined by the Bradford protein assay kit (Thermo Scientific, USA).

Animals

Specific pathogen-free (SPF grade) male C57BL/6 mice, weighing 18-20 g and aged 6 weeks, were purchased from Beijing HFK Bio-Technology Co., LTD. Mice were maintained in the Animal Center of Tongji Medical College of Huazhong University of Science and Technology. The investigation was approved by the Animal Care and Use Committee of Union Hospital of Huazhong University of Science and Technology and conformed to the Guide for the Care and Use of Laboratory Animals published by the US National Institutes of Health (NIH Publication No. 85-23, revised 1985).

The mice were randomly divided into the following four groups: the sham + VLP group ($n = 10$), the MI + VLP group ($n = 20$), the MI + ATRQβ-001 group ($n = 20$), and the MI + valsartan group ($n = 20$). MI was induced by ligating the left anterior descending (LAD) coronary artery on day 19. In the sham + VLP group, sham operation was performed without LAD ligation. The MI + ATRQβ-001 group was immunized subcutaneously on days 0, 14, 28, 56, and 84 with 100 μg of ATRQβ-001 vaccine formulated in aluminum hydroxide gel. The sham + VLP group and the MI + VLP group were vaccinated subcutaneously with 100 μg of Qβ-VLP formulated in aluminum hydroxide gel at the same time points. The MI + valsartan group was administered per oral valsartan (6 mg/kg/day, Norvatis) from days 14 to 103. The ATR-001-specific antibody titers were measured on days 0, 19, 33, 47, 68, 89, and 103 by enzyme-linked immunosorbent assay (ELISA).

ELISA

The ATRQβ-001 antibody titer was determined by ELISA. For each well of the 96-well plate, 1 μg of ATR-001 peptide was diluted in 100 μl of 0.1 M sodium bicarbonate solution pH 9.6 and incubated overnight at 4 °C. The plates were washed three times with phosphate-buffered saline (PBS + Tween-20 (PBST; 0.05% Tween-20) and then blocked with 1% bovine serum albumin (MP Biomedicals, LLC, Santa Ana, CA, USA) for 1 h at 37 °C. The plates were washed again three times with PBST and incubated with 100 μl blood samples at three different dilutions between 1:5000 and 1:20000 for 1 h at 37 °C. Nonimmune serum was used as a negative control. Following three washes with PBST, plates were incubated with 100 μl diluted horseradish peroxidase (HRP)-conjugated goat anti-mouse immunoglobulin G (IgG) (1:3000 dilution; Pierce; Thermo Fisher Scientific, Inc.) for 30 min at 37 °C. The reaction was developed by adding 100 μl 3,3′,5,5′-tetramethylbenzidine (Sigma-Aldrich; Merck KGaA) for 5 min at room temperature. Finally, 200 μl 1 M hydrochloric acid was added to stop the reaction, and the absorbance was determined at 450 nm using a BioTeck Epoch microplate reader.

Induction of MI and infarct size measurement

Mice were anesthetized with pentobarbital (70 mg/kg, i.p.) and ventilated with a small animal respirator (Harvard Apparatus, USA). A left thoracotomy was performed. The LAD coronary artery was ligatured to interrupt left coronary artery flow. For animals undergoing a sham operation, a ligature was placed in an identical location but not tied. The chest cavity was then closed in layers, and the animal was allowed to recover.

To measure the infarct size, the heart was frozen at −80 °C for 10 min and cut into slices (5-6 slices/heart), which were then incubated for 15 min in sodium phosphate buffer containing 1% TTC (2,3,5-triphenyl-tetrazolium chloride) to visualize the unstained infarcted region. Image-Pro Plus version 6.0 software (Media Cybernetics, MD) was used to determine the infarct size.

Terminal deoxynucleotidyl transferase dUTP nick end labeling (TUNEL) staining

To detect apoptosis, the paraffin-embedded heart sections were stained using the In Situ Cell Death Detection kit (Roche, Germany) according to the manufacturer's instructions. The sections should be incubated 15-30 min at 21-37 °C with proteinase K before staining. After washed in PBS, the section tissues were permeabilized in 0.1% Triton X-100 in sodium citrate. TUNEL reaction mix was added and incubated for 60 min at 37 °C in the dark. The nuclei were stained with 4′,6-diamidino-2-phenylindole. More than 10 fields (10 sections per mice) were examined in a blinded fashion by a technician who was not informed about the treatment groups.

Hemodynamic measurement

The systolic blood pressure (SBP) and heart rates of mice were detected using the tail-cuff method (BP-98A; Softron, Japan). The SBP was calculated from 10 to 15 readings for each mouse. All measurements were performed in a quiet environment at a temperature between 20 and 25 °C in a blinded manner.

Echocardiography

Echocardiography was performed on days 7, 28, and 84 after AMI. Mice were anesthetized with 1.5% isoflurane at the temperature of 36.5-37.5 °C. Images were obtained using a Vevo 2100 high-resolution imaging system equipped with a 30-MHz transducer (VisualSonics, Canada). All measurements were analyzed off-line by blinded observers using the Vevo 2100 workstation software. Each measurement reported was an average of ten cardiac cycles. LV end-diastolic diameter (LVIDED) and LV end-systolic diameter (LVIDES) were obtained from M-mode tracings from parasternal short-axis views at the mid and apical levels at each time point. Fractional shortening (FS) was calculated as % FS = (LVIDED-LVIDES)/LVIDED × 100%. Parasternal long-axis scans were used to provide additional data on LV end-diastolic volume (LVEDV) and LV end-systolic volume (LVESV). The formula of left ventricular ejection fraction (LVEF) percentage is [(EDV-ESV)/EDV] × 100%, (end-diastolic volume, EDV; end-systolic volume, ESV).

Plasma renin activity, Ang II, and aldosterone concentration measurement

The mice were decapitated between 9 am and 12 am at day 7 post MI. Blood samples were immediately collected and divided into two parts: one was mixed with the ice-cold enzyme inhibitor mixture (1 ml blood in 50 µl inhibitor mixture, including 20 µl 0.3 mol/l ethylenediaminetetraacetic acid, 10 µl 0.32 mol/l dimercaprol, and 20 µl 0.34 mol/l 8-OH-quinoline sulfate) for plasma renin activity (PRA) and Ang II measurement by radioimmunoassay (RIA) according to the assay kit instruction (NIBT, Beijing); the other was anticoagulated with ice-cold heparin for aldosterone measurement by RIA according to the assay kit instructions (NIBT, Beijing). The plasma was quickly separated to be tested in 4 °C. If the sample could not be detected immediately, it was stored at −20 °C as soon as possible. The actual measurement of the sample was performed in the laboratory of Nuclear Medicine Department in Union Hospital (Wuhan) in a blinded manner. For tissue Ang II measurement, immediately after harvesting and weighing, the hearts were immersed in ice-cold methanol, minced, and homogenized with tissue homogenizers. The homogenates were centrifuged (4000 rpm, 4 °C, 15 min), and the supernatants were dried overnight in a vacuum centrifuge. The dried residue was reconstituted in 1 ml RIA buffer and then was subjected to high-performance liquid chromatography to separate and measure Ang II (GL Biochem Ltd., Shanghai).

Histopathology and immunohistochemistry

The excised heart was routinely fixed in 4% phosphate-buffered paraformaldehyde and then embedded in paraffin for histologic staining. The fixed sections of the tissues were stained with hematoxylin and eosin (HE) and Masson's trichrome (Masson). Immunohistochemical staining was performed to detect macrophages (CD68, 1:100, AbD Serotec) in the junction between infarction and noninfarction regions. More than 10 fields (10 sections per animal) were examined in a blinded way.

Total RNA isolation and qRT-PCR analysis

Total RNA was extracted from the heart tissue by using the TRIzol Reagent (Invitrogen, USA) following the manufacturer's protocol. The cDNA was synthesized from 20 µl reverse transcription reaction (Takara, Japan) by using 1 µg total RNA. The expression of the associated genes was assessed using quantitative RT-PCR (qRT-PCR) performed with a Step One Real-Time PCR machine (Applied Biosystems, USA) using Platinum SYBR Green qPCR superMix-uracil-DNA glycosylase (Invitrogen, USA). Primers are shown in Supplementary table 1.

Western blotting

Protein extracted from heart tissues was separated on 10% sodium dodecyl sulphate-polyacrylamide gel electrophoresis and transferred to polyvinylidene difluoride membranes. After

being blocked with 5% skim milk, the membranes were incubated with the appropriate primary antibodies at 4 °C overnight, followed by incubation with an HRP-conjugated secondary antibody. The antigens were bound by the primary antibodies as follows: anti-NF-κB/p65 (CST, 8284), anti-VCAM-1 (Abcam, ab134047), anti-MCP-1 (Abcam, ab7202), anti-TGF-β1 (Abcam, ab6179965), anti-Bcl-2 (Abcam, ab32124), anti-Bax (Abcam, ab32053), anti-p-Smad2 (Arigo, ARG51796), anti-p-Smad3 (Arigo, ARG51797), anti-Smad2 (CST, 5339 S), anti-Smad3 (CST, 9523 S), anti-AT_1R (Abcam, ab124734), and anti-cleaved caspase-3 (Immunoway, YT6161). The specific bands were detected using Super ECL reagent (Thermo Scientific, USA). Images were obtained and analyzed with Image Lab 3.0 software (Bio-Rad, USA).

Statistical analysis

Data are presented as the means ± SEM. Differences were evaluated using one-way analysis of variance for multiple comparisons, followed by a post hoc Student-Newmann-Keuls test when necessary. Survival was analyzed by the Kaplan-Meier method with significant differences between the mortality curves assessed using the Breslow test. One-way repeated measures analysis of variance was used for analysis of SBP and heart rate. All analyses were done using GraphPad Prism 6.0 (GraphPad Software, CA), and statistical significance was set at $p < 0.05$.

Results

Animal characteristics

This study spans three periods of 1 week, 4 weeks, and 12 weeks after AMI in mice. The vaccine and valsartan were administered as shown in Fig. 1a. ELISA confirmed that the anti-ATR-001 peptide antibody titer was 1:60,000~1:120,000 after the second immunization (Fig. 1b), which indicated the high antigenicity of the ATR-001 epitope peptide. The SBP was not different among the groups in the early phase after AMI, but in contrast to the sham + VLP group, the SBP of the other three groups apparently decreased as the time went on, especially in the MI + ATRQβ-001 and MI + valsartan groups (Fig. 1c).

Animals were killed on days 26, 47, and 103. Supplementary table 2 presents the characteristics of animals in the study. There were no significant differences for the body weight and heart rate among the experimental groups. However, the ratio of heart weight to body weight was significantly higher in the MI subgroup compared with the sham + VLP group ($p < 0.001$).

ATRQβ-001 vaccine improved survival rate and heart function

Fig. 2a shows survival curves of the four groups. There were nine, four, and six deaths after surgery in the MI + VLP, MI + ATRQβ-001, and MI + valsartan groups, respectively. The post-MI survival rate was 55% in the MI + VLP group, 80% in the ATRQβ-001 vaccine group, and 70% in the valsartan group, indicating that the ATRQβ-001 vaccine dramatically decreased post MI mortality (compared with MI + VLP, 80% versus 55%, mean estimate (days) 68.4 ± 7.0 versus 47.8 ± 8.9, $p = 0.046$).

To verify the effect of the ATRQβ-001 vaccine on cardiac function after infarction, the cardiac function was observed on days 7, 28, and 84 after MI. First, the infarct size was assessed on day 7 after MI. TTC staining of the heart tissue sections was used to distinguish between infarct and non-infarct areas. The MI + ATRQβ-001 group and the MI + valsartan group showed similarly decreased infarct size compared to the MI + VLP group, although there was no significant difference (Fig. 2b). Echocardiographic data obtained on days 7, 28, and 84 following AMI are shown in Fig. 2 and Supplementary figure 1. LVEF and LVFS were significantly improved in the MI + ATRQβ-001 and MI + valsartan groups compared with the MI + VLP group. LVEF and LVFS of the MI + ATRQβ-001 group were higher than those of the MI + valsartan group at 7 days after AMI ($p = 0.032$, Fig. 2c, d). Secondary to cardiac ischemia, the LV volume and diameter (as shown by LVEDV and LVEDD) were increased in all three MI groups. However, although the LVEDV and LVEDD were ameliorated in the MI + ATRQβ-001 and MI + valsartan groups compared with the MI + VLP group, the difference was not significant except on day 28 (Fig. 2e, f, and Supplementary figure 1).

ATRQβ-001 vaccine mitigated inflammation

The activation of inflammation has a critical role in the progression of AMI [10, 11], especially in the early phase of AMI. CD68, as a surface marker of macrophages, was used to detect the macrophage infiltration in the myocardium at 7 days post MI. In contrast to the MI + VLP group, the number of macrophages in the MI + ATRQβ-001 group was obviously reduced (Fig. 3a, b), whereas there was no significant difference in the valsartan group (Fig. 3a, b). Meanwhile, both western blotting and qRT-PCR demonstrated that the expression of NF-κB/p65 was dramatically attenuated in the MI + ATRQβ-001 group compared with the MI + VLP group (Fig. 3c-e). Similar results were also observed in the MI + valsartan group (Fig. 3c-e). In addition, compared with the MI + VLP group, the ATRQβ-001 vaccine decreased the expression of pro-inflammatory cytokines MCP-1, IL-1β, IL-6, IL-17A, TNF-α, and

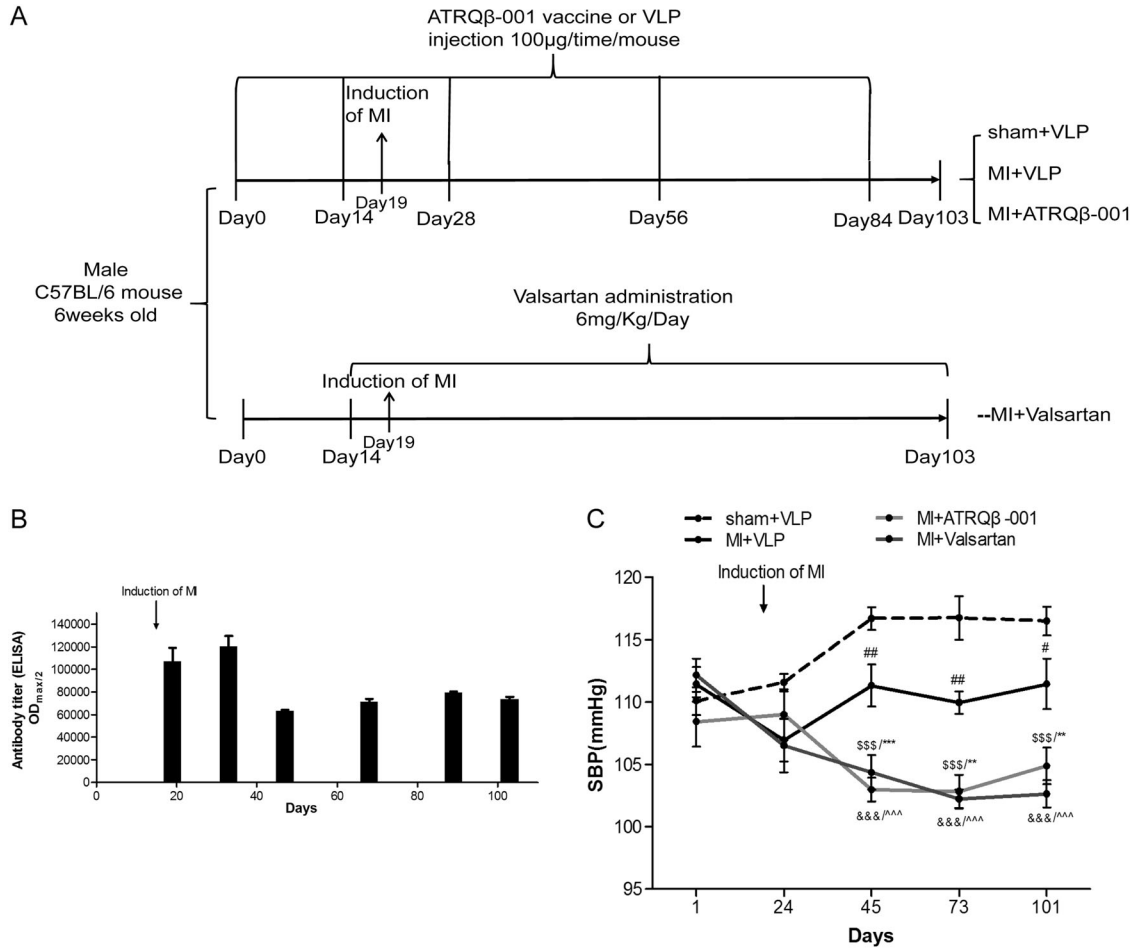

Fig. 1 Animal characteristics. **a** The protocols of vaccination and valsartan administration for 103 days. **b** The serum anti-ATRQβ-001 vaccine antibody titer in the MI + ATRQβ-001 group. **c** The SBP of four groups. VLP, virus-like particles; SBP, systolic blood pressure. $^{\#}p < 0.05$, $^{\#\#}p < 0.01$, $^{**}p < 0.01$, $^{***}p < 0.001$, $^{\$\$\$}p < 0.001$, $^{\&\&\&}p < 0.001$, $^{\wedge\wedge\wedge}p < 0.001$, $^{\#}$versus sham + VLP, *versus MI + VLP, $^{\$}$MI + ATRQβ-001 versus sham + VLP, & MI + valsartan versus sham + VLP, $^{\wedge}$MI + valsartan versus MI + VLP

VCAM-1, whereas increasing the expression of anti-inflammatory cytokines TGF-β and IL-10 post MI (Fig. 3c-e). The IL-10 level of the ATRQβ-001 vaccine group was more abundant than that of the valsartan group at 7 day after AMI (Fig. 3e). In the late phase of AMI, the ATRQβ-001 vaccine just slightly mitigated inflammation post MI (Supplementary figure 2).

ATRQβ-001 vaccine inhibited apoptosis

Apoptosis is also involved in the progression of AMI [12]. TUNEL assays were carried out to detect apoptosis after AMI. As shown in Fig. 4a, b, both the ATRQβ-001 vaccine and valsartan manifestly inhibited apoptosis compared to the MI + VLP group. To further confirm the effect, the protein and mRNA expression of apoptosis-associated molecules Bax and Bcl-2 was detected. Compared with the MI + VLP group, ATRQβ-001, and valsartan markedly decreased the expression of Bax and relatively increased the expression of Bcl-2, indicating a higher ratio of Bcl-2/Bax in the MI + ATRQβ-001 and MI + valsartan groups (Fig. 4c-e). In addition, the ATRQβ-001 vaccine significantly inhibited the expression of cleaved caspase-3 (Supplementary figure 3).

ATRQβ-001 vaccine decreased myocardial fibrosis

Ventricular remodeling as an inevitable process after AMI tightly affects the prognosis, in which the most common and most important is myocardial fibrosis. Masson staining was used to measure the myocardial fibrosis on days 28 and 84 after AMI. The results are shown in Fig. 5a, b; ATRQβ-001 and valsartan obviously inhibited the myocardial fibrosis compared with the MI + VLP group (64.5 ± 3.8% versus 78.6 ± 2.5%, $p < 0.001$; 72.0 ± 1.8% versus 78.6 ± 2.5%, $p < 0.001$). The ATRQβ-001 vaccine decreased myocardial fibrosis more than valsartan (64.5 ± 3.8% versus 72.0 ± 1.8%, $p < 0.001$).

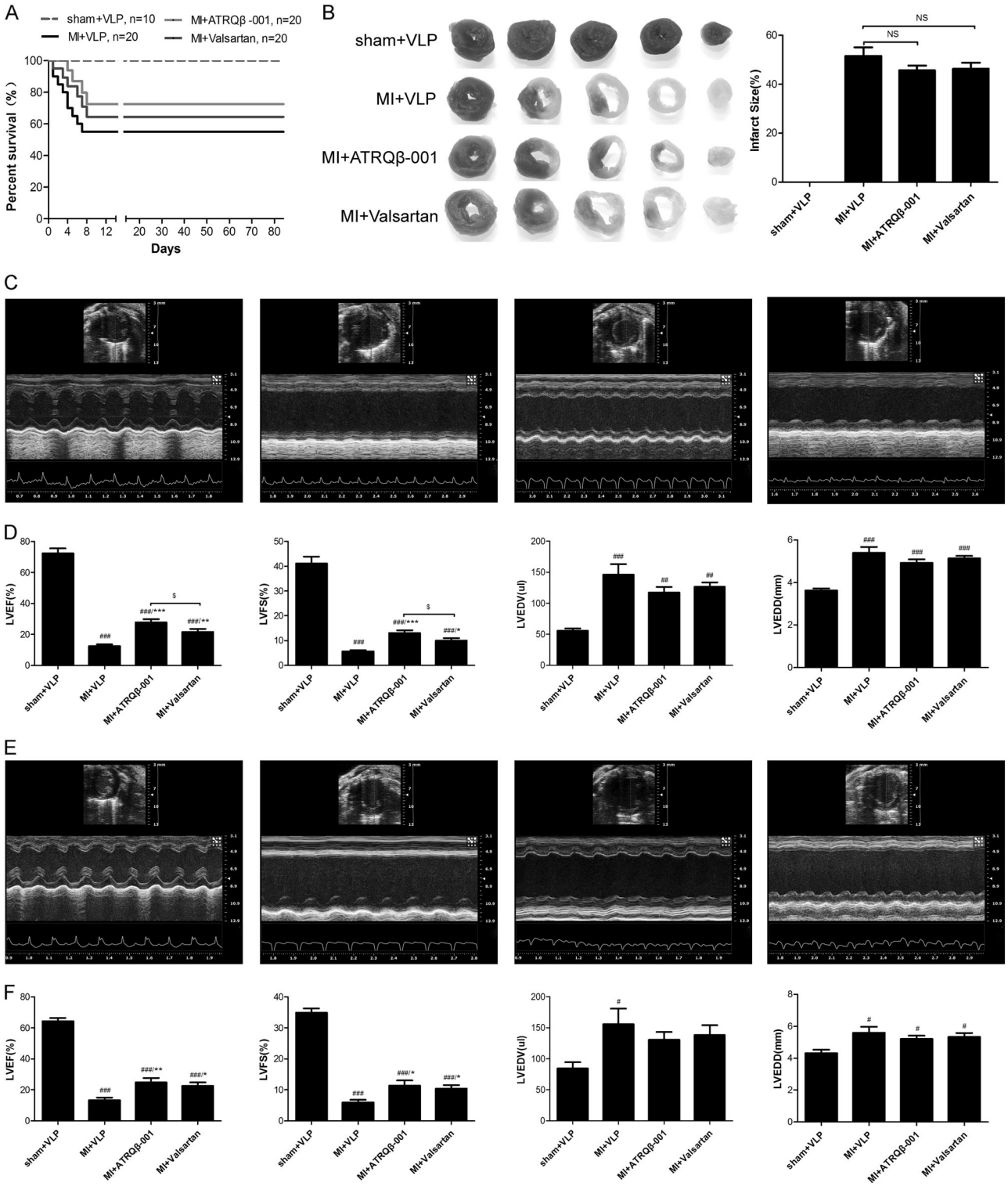

Fig. 2 ATRQβ-001 vaccine improved survival rate and cardiac function. **a** Survival analysis for 84 days. **b** Infarct size determined by TTC staining on day 7 post MI ($n = 5$). **c** Representative M-mode echocardiography images of the left ventricle on day 7 post MI. **d** LVEF, FS, LVEDV, and LVEDD on day 7 post MI (sham + VLP, $n = 5$; MI + VLP, $n = 11$; MI + ATRQβ-001, $n = 19$; MI + valsartan, $n = 11$). **e** Representative M-mode echocardiography images of the left ventricle on day 84 post MI. **f** LVEF, FS, LVEDV, and LVEDD on day 84 post MI (sham + VLP, $n = 5$; MI + VLP, $n = 5$; MI + ATRQβ-001, $n = 6$; MI + valsartan, $n = 5$). VLP, virus-like particles; TTC: 2, 3,5-triphenyltetrazolium chloride; LVEF, left ventricular ejection fraction; LVFS, Left ventricular fractional shortening; LVEDV, left ventricular end-diastolic volume; LVEDD, left ventricular end-diastolic diameter. $^{\#}p < 0.05$, $^{\#\#}p < 0.01$, $^{\#\#\#}p < 0.001$, $^{*}p < 0.05$, $^{**}p < 0.01$, $^{***}p < 0.001$, $^{\$}p < 0.05$, $^{\#}$versus sham + VLP, *versus MI + VLP, $^{\$}$versus MI + ATRQβ-001

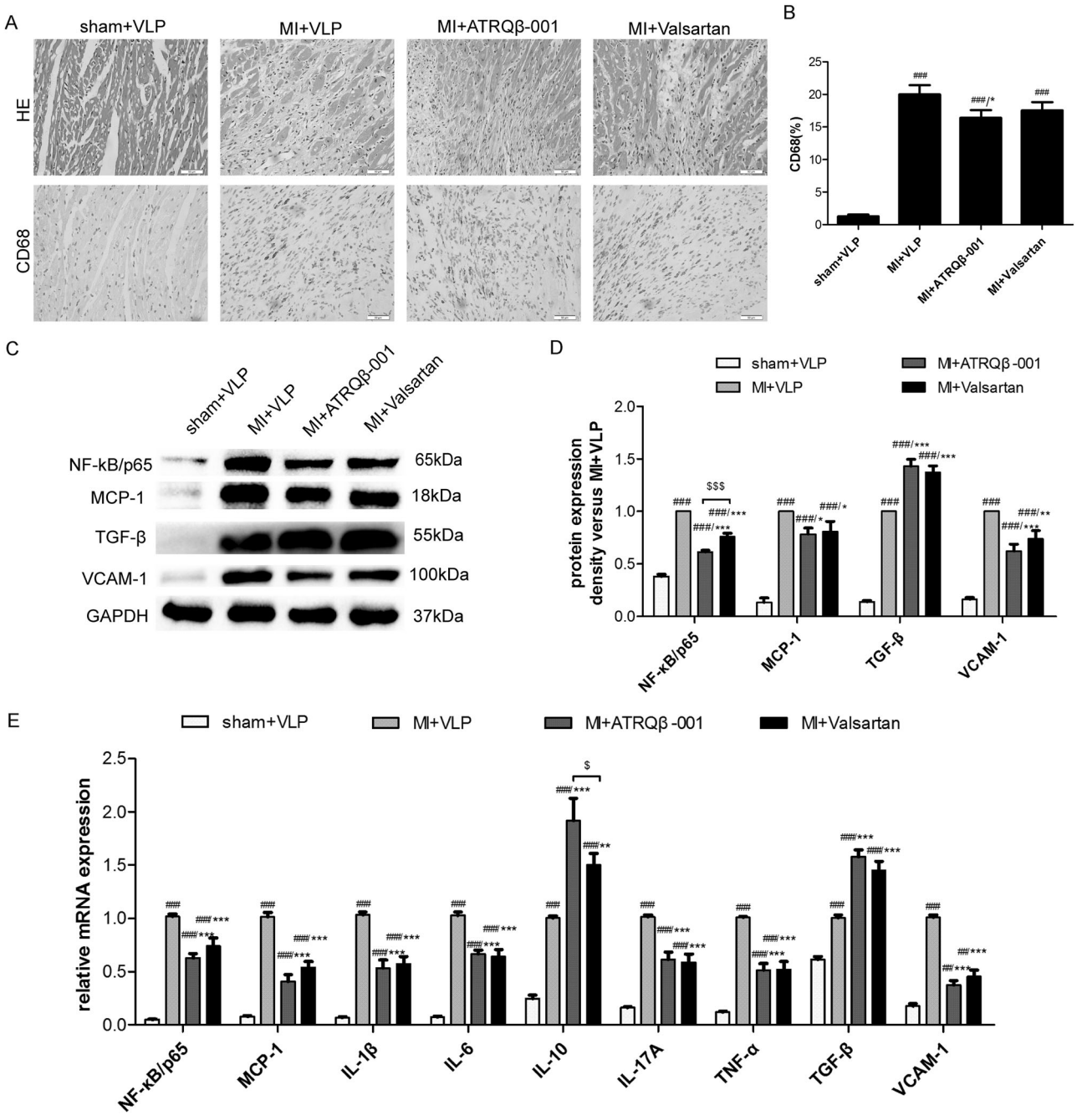

Fig. 3 ATRQβ-001 vaccine mitigated inflammation. **a** Representative images of HE staining and infiltration of CD68 macrophages in the border area of the infarct hearts on day 7 post MI ($n = 3$). **b** Quantitative analysis of macrophage infiltration in the four groups on day 7 post MI. **c**, **d** Western blot analysis of NF-κB/p65, MCP-1, TGF-β, and VCAM-1 protein levels in the border area of the infarct hearts. GAPDH was a loading control. **e** mRNA level analysis of NF-κB/p65, MCP-1, IL-1β, IL-6, IL-17A, TNF-α, VCAM-1, IL-10, and TGF-β on day 7 after AMI. VLP, virus-like particles; HE, hematoxylin and eosin; NF-κB, Nuclear factor-κB; MCP-1, monocyte chemotactic protein 1; TGF-β, transforming growth factor-β; IL, interleukin; TNF-α, tumor necrosis factor-α; VCAM-1, vascular cell adhesion molecule 1; GAPDH, Glyceraldehyde-3-phosphate dehydrogenase. Data are depicted as fold changes versus MI + VLP. $^{\#}p < 0.05$, $^{\#\#}p < 0.01$, $^{\#\#\#}p < 0.001$, $^{*}p < 0.05$, $^{**}p < 0.01$, $^{***}p < 0.001$, $^{\$}p < 0.05$, $^{\$\$}p < 0.01$, $^{\$\$\$}p < 0.001$, $^{\#}$versus sham + VLP, *versus MI + VLP, $^{\$}$versus MI + ATRQβ-001. Scale bar = 50 μm

The activation of the TGF-β1/Smad2-3 signaling pathway promotes fibrosis [3, 13]. Our result showed that the protein and mRNA expression levels of TGF-β1 and Smad2/3 were prominently decreased in the ATRQβ-001 and valsartan groups in comparison with the MI + VLP group (Fig. 5c-e). Similarly, the expression of collagen-I and collagen-III was also reduced significantly in the MI + ATRQβ-001 and MI + valsartan groups compared with the

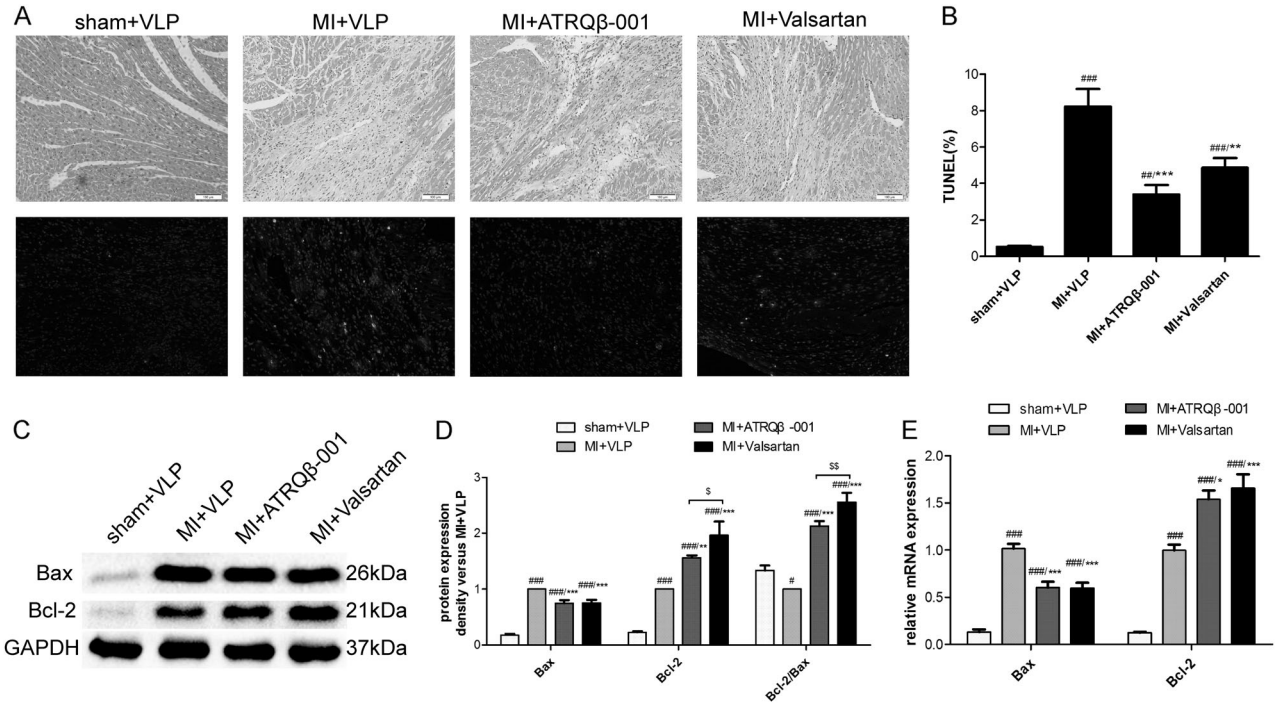

Fig. 4 ATRQβ-001 vaccine inhibited apoptosis. **a** Representative images of HE staining and TUNEL staining on day 7 post MI. TUNEL (green) and 4,6-diamidino-2-phenylindole (blue) staining of nuclei in the peri-infarct zone. **b** Quantitative analysis of the TUNEL-positive nuclei ($n = 3$). **c**, **d** Western blot analysis of Bax and Bcl-2 protein levels in the peri-infarct zone. GAPDH was a loading control. **e** mRNA level analysis of Bax and Bcl-2 on day 7 post MI. VLP, virus-like particles; HE, hematoxylin and eosin; TUNEL, terminal dUTP-biotin nick end labeling; GAPDH, Glyceraldehyde-3-phosphate dehydrogenase. Data are depicted as fold changes versus MI + VLP. $^{\#}p < 0.05$, $^{\#\#}p < 0.01$, $^{\#\#\#}p < 0.001$, $^{*}p < 0.05$, $^{**}p < 0.01$, $^{***}p < 0.001$, $^{\$}p < 0.05$, $^{\#}$versus sham + VLP, *versus MI + VLP, $^{\$}$versus MI + ATRQβ-001. Scale bar = 100 μm

MI + VLP group (Fig. 5e and Supplementary figure 4). The expression of prepro-BNP was also detected; however, the ATRQβ-001 vaccine did not decrease the level of myocardial prepro-BNP on days 7, 28, and 84 post MI (Supplementary figure 5).

ATRQβ-001 vaccine decreased cardiac Ang II concentration with no feedback of RAS

To assess the effect of the ATRQβ-001 vaccine on circulating RAS, we detected the PRA, Ang II, and aldosterone concentration. Circulating RAS and heart Ang II levels were increased in all MI subgroups. The PRA in the MI + ATRQβ-001 group was similar to that of the MI + VLP group ($p = 0.689$). However, a distinct increase was observed in the MI + valsartan group (7.3 ± 2.4 ng/ml/h) compared with the MI + ATRQβ-001 group and the MI + VLP group ($p < 0.01$; Fig. 6a). Similarly, the plasma concentration of Ang II was higher in the MI + valsartan group than in the MI + ATRQβ-001 group (643.3 ± 159.1 versus 371.0 ± 127.8 pg/ml, $p = 0.001$; Fig. 6b). Both the MI + valsartan group and the MI + ATRQβ-001 group had decreased plasma aldosterone concentrations compared with the MI + VLP group (Fig. 6c). To further examine the local RAS, heart Ang II concentration was measured. The concentration of Ang II in hearts was lower in both the ATRQβ-001 group and the valsartan group (Fig. 6d).

ATRQβ-001 vaccine downregulated the expression of AT_1R

To further find the effect of the ATRQβ-001 vaccine on AT_1R, the protein and mRNA expression levels of AT_1R were determined on days 7, 28, and 84 after AMI. In comparison with the MI + VLP group, neither the ATRQβ-001 vaccine nor valsartan had significant effects on the expression of AT_1R at 7 days after AMI (Fig. 7a-c). However, both the ATRQβ-001 vaccine and valsartan evidently decreased the expression of AT_1R on days 28 and 84 after AMI (Fig. 7a-c).

Discussion

Adverse ventricular remodeling after AMI precipitates an impaired ventricular function and heart failure, leading to increased morbidity and mortality. Our study showed that

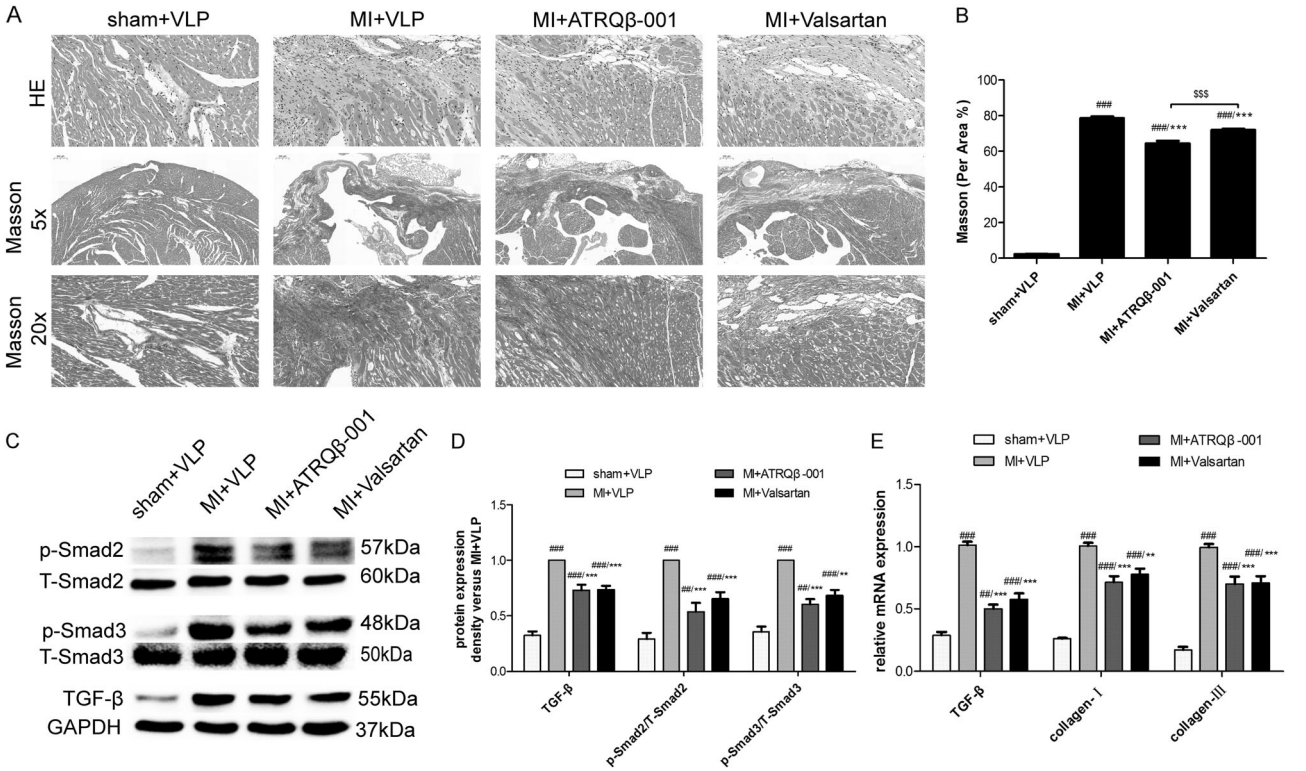

Fig. 5 ATRQβ-001 vaccine decreased myocardial fibrosis. **a** Representative images of HE staining and Masson's trichrome staining in whole hearts. **b** Quantitative analysis of myocardial fibrosis ($n = 3$). **c**, **d** Western blot analysis of TGF-β, p-Smad2, T-Smad2, p-Smad3, and T-Smad3 protein level. GAPDH was a loading control. **e** mRNA level analysis of TGF-β, collagen-I, and collagen-III on day 84 post MI. VLP, virus-like particles; HE, hematoxylin and eosin; GAPDH, Glyceraldehyde-3-phosphate dehydrogenase; TGF-β, transforming growth factor-β. Data are depicted as fold changes versus MI + VLP. $^{\#\#}p < 0.01$, $^{\#\#\#}p < 0.001$, $^{**}p < 0.01$, $^{***}p < 0.001$, $^{\$\$\$}p < 0.001$, $^{\#}$versus sham + VLP, *versus MI + VLP, $^{\$}$versus MI + ATRQβ-001. HE, Masson × S20 scale bar = 50 μm; Masson × 5 scale bar = 200 μm

the ATRQβ-001 vaccine obviously improved postinfarct survival and prevented cardiac remodeling after AMI.

Persistent inflammatory responses participate in the early phase of adverse ventricular remodeling after AMI, including the pro-inflammatory and anti-inflammatory factors. Controlled inflammation and immune response are prerequisites for adequate cardiac healing after AMI [14]. Xia et al. [15] reported that IL-17A has a pathogenic role in myocardial ischemia/reperfusion injury by inducing cardiomyocyte apoptosis and neutrophil infiltration. Other classical inflammatory cytokines, such as MCP-1, IL-1β, IL-6, TNF-α, and VCAM-1, are generally accepted to promote inflammatory cell infiltration and tissue damage after AMI. To counteract the effect of pro-inflammatory factors, some anti-inflammatory cytokines were also produced. The classical factors are TGF-β and IL-10, which negatively regulate post-MI immune injury [16, 17]. Dimmeler et al. [18] and Kishore et al. [19] showed that exogenous administration of IL-10 attenuated ventricular remodeling after AMI. In this study, the number of macrophages infiltrating into the myocardium in the ATRQβ-001 group was obviously reduced. The production of inflammatory cytokines, such as NF-κB/p65, MCP-1, IL-1β, IL-6, IL-17A, TNF-α, and VCAM-1, was significantly attenuated after AMI in the ATRQβ-001 group. Furthermore, the ATRQβ-001 vaccine dramatically increased IL-10 expression in the infarcted heart. The level of IL-10 was more abundant in the ATRQβ-001 group than in the valsartan group. These indicated that the ATRQβ-001 vaccine had the ability to control inflammation and immune response after AMI.

TGF-β, a multifunctional polypeptide, has an important role in the pathogenesis of cardiac remodeling and fibrosis [20, 21]. TGF-β has been shown to downregulate inflammatory cytokine production in monocytes and macrophages, likely by the inhibition of NF-κB [22]. In a mouse model of nonreperfused myocardial infarction, early systemic inhibition of TGF-β signaling through transfection with the extracellular domain of TβRII increased mortality by accentuating neutrophil recruitment and increasing expression of TNF-α, IL-1, and MCP-1/CCL2 [23]. The study also suggested that injection of exogenous TGF-β in isolated perfused hearts undergoing brief myocardial ischemia followed by reperfusion exerted protective actions by attenuating oxidative stress and reducing the release of pro-inflammatory cytokines [24]. These observations are consistent with an important role for TGF-β in negative

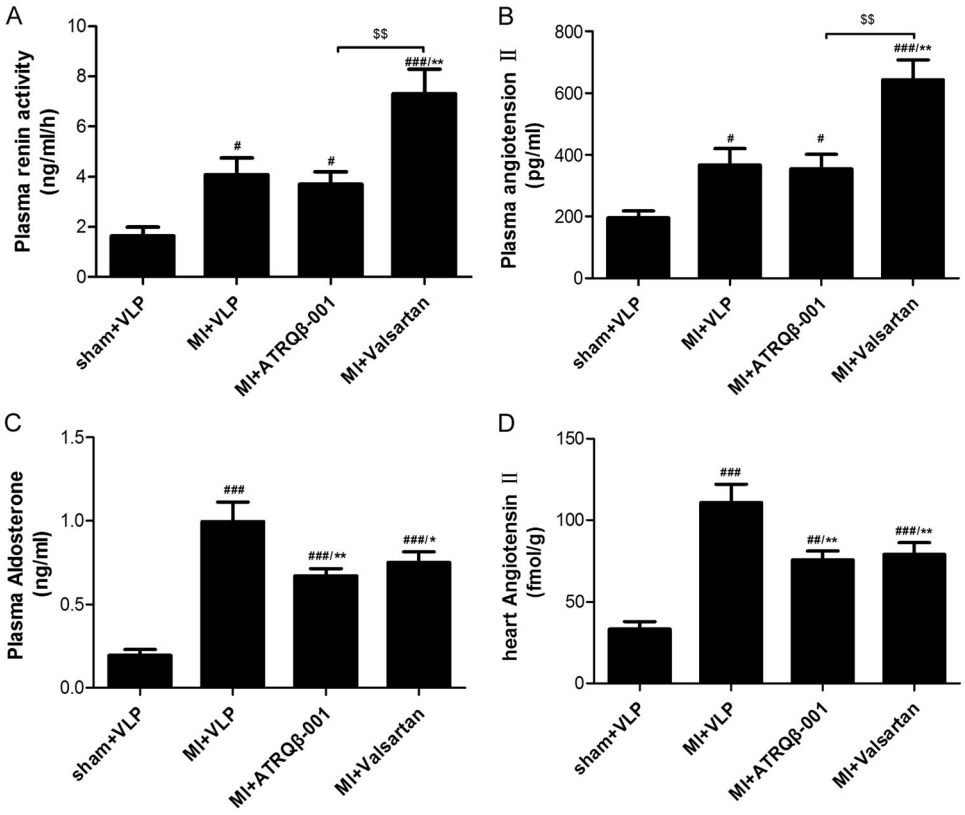

Fig. 6 ATRQβ-001 vaccine decreased cardiac Ang II concentration with no feedback of RAS. **a**-**c** Measurement of plasma renin activity (PRA), angiotensin II (Ang II), and aldosterone concentration. **d** Measurement of heart Ang II concentration. VLP, virus-like particles. $^{\#\#}p < 0.01$, $^{\#\#\#}p < 0.001$, $^{*}p < 0.05$, $^{**}p < 0.01$, $^{***}p < 0.001$, $^{\$\$\$}p < 0.001$, $^{\#}$versus sham + VLP, *versus MI + VLP, $^{\$}$versus MI + ATRQβ-001

regulation of the postinfarction inflammatory response in the early phase of AMI. Similarly, our vaccine may reduce inflammation by increasing TGF-β acting as a negative inflammatory regulator in the early phase of AMI. However, TGF-β1 also has a key role in activating a pro-fibrotic and matrix-preserving program in infarct fibroblasts through Smad-dependent actions following the progress of post-MI remodeling in the late phase of AMI [25, 26]. That is, TGF-β1 may serve as the master switch regulating the transition from inflammation to fibrosis [27]. Our result showed that the ATRQβ-001 vaccine significantly attenuated myocardial fibrosis. The expression of TGF-β1 and Smad2/3 was prominently decreased in the ATRQβ-001 group in the late phase of AMI. The expression of collagen-I and collagen-III was also reduced in the ATRQβ-001 group. Therefore, the ATRQβ-001 vaccine could likely lighten myocardial fibrosis, in part by regulating TGF-β1 in the different phase of AMI.

RAS plays an important role in the initiation and progression of tissue injuries in the cardiovascular system. The activation of Ang II/AT1R contributes to tissue injury via inflammation and pathologic remodeling after AMI. Our result showed that valsartan raised an obvious feedback of plasma RAS, whereas the ATRQβ-001 vaccine did not. However, heart tissue Ang II concentration was decreased in both groups. Further, in this study, the ATRQβ-001 vaccine evidently decreased the expression of AT_1R at weeks 4 and 12 after AMI. These indicated that the ATRQβ-001 vaccine might have a different mechanism, unlike valsartan. It has been reported that Ang II binding with the AT_1R increases the accessibility of ^{181}Ala, ^{182}Phe, and ^{183}His, which belong to the AT_1R ECL2 region [28]. This conformational change is followed by AT_1R activation. Interestingly, the target peptide of the ATRQβ-001 vaccine is 181–187 amino acid residues of AT_1R ECL2. The ATRQβ-001 vaccine antibody may block Ang II-induced AT_1R activation through binding to the AT_1R ECL2 region that includes ^{181}Ala, ^{182}Phe, and ^{183}His. Meanwhile, according to our previous work, the ATRQβ-001 vaccine antibody and Ang II did not competitively bind to AT_1R [7]. That is, the antibody and Ang II may have different binding sites with AT_1R. Moreover, recent studies suggested that AT_1R possesses a biased signaling pathway, such as the classical arrestin pathway-selective agonist [Sar^1-Ile^4-Ile^8]Ang II (SII) [29, 30]. Thus, we speculate that the ATRQβ-001 vaccine may be a biased regulator of AT_1R, different from the overall blocking of ARB. These could be the potential mechanisms by which the ATRQβ-001 vaccine does not provoke the activation of circulating RAS. Further investigation is needed in the future.

Compared with per oral chemical drugs, the ATRQβ-001 vaccine has potential superiority, including the effect of stability and great improvement in patient compliance. In addition, no obvious feedback activation of circulating or

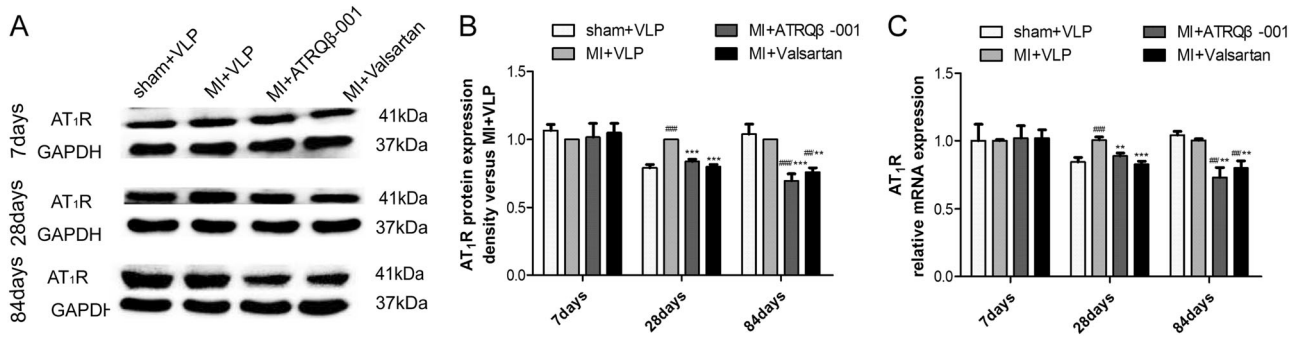

Fig. 7 ATRQβ-001 vaccine downregulated the expression of AT_1R. **a**, **b** Western blot analysis of AT_1R protein level on days 7, 28, and 84 post MI. GAPDH was a loading control. **c** mRNA level analysis of AT_1R on days 7, 28, and 84 post MI. VLP, virus-like particles; AT_1R, angiotensin II type 1 receptor; GAPDH, Glyceraldehyde-3-phosphate dehydrogenase. Data are depicted as fold changes versus MI + VLP. $^{\#\#}p < 0.01$, $^{\#\#\#}p < 0.001$, $^{**}p < 0.01$, $^{***}p < 0.001$, $^{\#}$versus sham + VLP, *versus MI + VLP

local RAS was observed in the ATRQβ-001 vaccine group, which is one of the prominent characteristics of the vaccine. These advantages of the ATRQβ-001 vaccine may provide better heart protection after AMI. In our study, the improvement of survival, cardiac inflammation infiltration and remodeling with the ATRQβ-001 vaccine was slightly superior to that of the valsartan group. However, longer observation is needed to distinguish the difference between the ATRQβ-001 vaccine and ARBs. Recently, Watanabe R et al. [31] showed that vaccination against Ang II attenuates the cardiac dysfunction induced by myocardial infarction. Similar to the CYT-006-AngQβ vaccine [32], they are both against Ang II (ligand), and vaccination with the Ang II vaccine led to the significant increase of plasma Ang II (feedback activation of RAS), whereas the ATRQβ-001 vaccine targets AT_1R (Ang II receptor) and does not cause feedback activation of RAS. To our knowledge, the elevated Ang II can be converted to Ang IV under the action of aminopeptidase A and aminopeptidase M. Ang IV activates insulin-regulated aminopeptidase receptor and then promotes the release and activation of pro-inflammatory and procoagulant factors (such as PAI-1), which ultimately aggravate vascular remodeling and thrombogenesis [33]. The feedback activation of RAS in the Ang II vaccine may cripple the target organ protection to some extent on AMI. Compared with the Ang II vaccine, the ATRQβ-001 vaccine may provide better protection of target organs.

The safety of the ATRQβ-001 vaccine is an important consideration. Peptide-VLP hypertension vaccine (CYT-006-AngQβ) showed good safety in clinical trials [32]. Our ATRQβ-001 vaccine has been sufficiently demonstrated to be safe in a series of studies [7–9]. Further, the immune response mechanism of peptide-VLP vaccine has been elucidated in our previous work, which indicated that the peptide-VLP vaccine has satisfactory safety [34]. In conclusion, the ATRQβ-001 vaccine obviously improved post MI survival and prevented cardiac remodeling after AMI in mice. The ATRQβ-001 vaccine may be a novel approach for treating ventricular remodeling after AMI.

Acknowledgements

Funding This work was supported by the Major Research Plan of the National Natural Science Foundation of China (No. 91439207) and the National Natural Science Foundation of China (No. 81400314, No. 81500388, No. 31370931, No. 81470494).

Compliance with ethical standards

Conflict of interest The authors declare that they have no conflict of interest.

References

1. Pfeffer MA, Braunwald E. Ventricular remodeling after myocardial infarction: experimental observations and clinical implications. Circulation. 1990;81:1161–72.
2. Sui X, Wei H, Wang D. Novel mechanism of cardiac protection by valsartan: synergetic roles of TGF-β1 and HIF-1α in Ang II-mediated fibrosis after myocardial infarction. J Cell Mol Med. 2015;19:1773–82.
3. Prabhu SD, Frangogiannis NG. The biological basis for cardiac repair after myo-cardial infarction: from inflammation to Fibrosis. Circ Res. 2016;119:91–112.
4. Bujak M, Ren G, Kweon HJ, Dobaczewski M, Reddy A, Taffet G, et al. Essential role of Smad3 in infarct healing and in the pathogenesis of cardiac remodeling. Circulation. 2007;116:2127–38.
5. Strauss MH, Hall AS. Angiotensin-converting enzyme inhibitors and angiotensin II receptor antagonists in the treatment of heart failure caused by left ventricular systolic dysfunction. Prog Cardiovasc Dis. 2016;58:473–82.
6. Vijan SG. Angiotensin-converting enzyme inhibitors (ACEIs), not angiotensin receptor blockers (ARBs), are preferred and effective mode of therapy in high cardiovascular risk patients. J Indian Med Assoc. 2009;107:178–82.
7. Chen X, Qiu Z, Yang S, Ding D, Chen F, Zhou Y, et al. Effectiveness and safety of a terapeutic vaccine against angiotensin II receptor type 1 in hypertensive animals. Hypertension. 2013;61:408–16.

8. Zhou Y, Wang S, Qiu Z, Song X, Pan Y, Hu X, et al. ATRQβ-001 vaccine prevents atherosclerosis in apolipoprotein E-null mice. J Hypertens. 2016;34:474–85.
9. Ding D, Du Y, Qiu Z, Yan S, Chen F, Wang M, et al. Vaccination against type 1 angiotensin receptor prevents streptozotocin-induced diabetic nephropathy. J Mol Med (Berl). 2016;94:207–18.
10. Nian M, Lee P, Khaper N, Liu P. Inflammatory cytokines and postmyocardial infarction remodeling. Circ Res. 2004;94:1543–53.
11. Frangogiannis NG. Targeting the inflammatory response in healing myocardial infarcts. Curr Med Chem. 2006;13:1877–93.
12. Hojo Y, Saito T, Kondo H. Role of apoptosis in left ventricular remodeling after acute myocardial infarction. J Cardiol. 2012; 60:91–2.
13. Su SA, Yang D, Wu Y, Xie Y, Zhu W, Cai Z, et al. EphrinB2 regulates cardiac fibrosis through modulating the interaction of Stat3 and TGF-β/Smad3 signaling. Circ Res. 2017;121:617–27.
14. Zhu R, Sun H, Yu K, Zhong Y, Shi H, Wei Y, et al. Interleukin-37 and dendritic cells treated with interleukin-37 plus troponin I ameliorate cardiac remodeling after myocardial infarction. J Am Heart Assoc. 2016;5:e004406.
15. Liao YH, Xia N, Zhou SF, Tang TT, Yan XX, Lv BJ, et al. Interleukin-17A contributes to myocardial ischemia/reperfusion injury by regulating cardiomyocyte apoptosis and neutrophil infiltration. J Am Coll Cardiol. 2012;59:420–9.
16. Tang TT, Yuan J, Zhu ZF, Zhang WC, Xiao H, Xia N, et al. Regulatory T cells ameliorate cardiac remodeling after myocardial infarction. Basic Res Cardiol. 2012;107:232.
17. Jung M, Ma Y, Iyer RP, DeLeon-Pennell KY, Yabluchanskiy A, Garrett MR, et al. IL-10 improves cardiac remodeling after myocardial infarction by stimulating M2 macrophage polarization and fibroblast activation. Basic Res Cardiol. 2017;112:33.
18. Burchfield JS, Iwasaki M, Koyanagi M, Urbich C, Rosenthal N, Zeiher AM, et al. Interleukin-10 from transplanted bone marrow mononuclear cells contributes to cardiac protection after myocardial infarction. Circ Res. 2008;103:203–211.
19. Krishnamurthy P, Rajasingh J, Lambers E, Qin G, Losordo DW, Kishore R. IL-10 inhibits inflammation and attenuates left ventricular remodeling after myocardial infarction via activation of STAT3 and suppression of HuR. Circ Res. 2009;104:e9–18.
20. Bujak M, Frangogiannis NG. The role of TGF-β signaling in myocardial infarction and cardiac remodeling. Cardiovasc Res. 2007;74:184–95.
21. Dobaczewski M, Chen W, Frangogiannis NG. Transforming growth factor (TGF)-β signaling in cardiac remodeling. J Mol Cell Cardiol. 2011;51:600–6.
22. Smythies LE, Sellers M, Clements RH, Mosteller-Barnum M, Meng G, Benjamin WH, et al. Human intestinal macrophages display profound inflammatory anergy despite avid phagocytic and bacteriocidal activity. J Clin Invest. 2005;115:66–75.
23. Ikeuchi M, Tsutsui H, Shiomi T, Matsusaka H, Matsushima S, Wen J, et al. Inhibition of TGF-beta signaling exacerbates early cardiac dysfunction but prevents late remodeling after infarction. Cardiovasc Res. 2004;64:526–35.
24. Lefer AM, Tsao P, Aoki N, Palladino MA Jr.. Mediation of cardioprotection by transforming growth factor-beta. Science. 1990;249:61–4.
25. Shinde AV, Frangogiannis NG. Fibroblasts in myocardial infarction: a role in inflammation and repair. J Mol Cell Cardiol. 2014;70:74–82.
26. Hao J, Ju H, Zhao S, Junaid A, Scammell-La Fleur T, Dixon IM. Elevation of expression of Smads 2, 3, and 4, decorin and TGF-beta in the chronic phase of myocardial infarct scar healing. J Mol Cell Cardiol. 1999;31:667–78.
27. Mehta JL, Chen HJ, Li DY. Protection of myocytes from hypoxia-reoxygenation injury by nitric oxide is mediated by modulation of transforming growth factor-beta1. Circulation. 2002;105:2206–11.
28. Unal H, Jagannathan R, Bhat MB, Karnik SS. Ligand-specific conformation of extracellular Loop-2 in the angiotensin II type 1 receptor. J Biol Chem. 2010;285:16341–50.
29. Wilson PC, Lee MH, Appleton KM, El-Shewy HM, Morinelli TA, Peterson YK, et al. The arrestin-selective angiotensin AT1 receptor agonist [Sar1,Ile4,Ile8]-AngII negatively regulates bradykinin B2 receptor signaling via AT1-B2 receptor heterodimers. J Biol Chem. 2013;288:18872–84.
30. Kendall RT, Lee MH, Pleasant DL, Robinson K, Kuppuswamy D, McDermott PJ, et al. Arrestin-dependent angiotensin AT1 receptor signaling regulates Akt and mTor-mediated protein synthesis. J Biol Chem. 2014;289:26155–66.
31. Watanabe R, Suzuki JI, Wakayama K, Maejima Y, Shimamura M, Koriyama H, et al. A peptide vaccine targeting angiotensin II attenuates the cardiac dysfunction induced by myocardial infarction. Sci Rep. 2017;7:43920.
32. Tissot AC, Maurer P, Nussberger J, Sabat R, Pfister T, Ignatenko S, et al. Effect of immunization against angiotensin II with CYT006-AngQb on ambulatory blood pressure: a doubleblind, randomised, placebo-controlled phase IIa study. Lancet. 2008; 371:821–7.
33. Fogari R, Zoppi A, Mugellini A, Maffioli P, Lazzari P, Derosa G. Role of angiotensin II in plasma PAI-1 changes induced by imidapril or candesartan in hypertensive patients with metabolic syndrome. Hypertens Res. 2011;34:1321–6.
34. Hu X, Deng Y, Chen X, Zhou Y, Zhang H, Wu H, et al. Immune response of a novel ATR-AP205-001 conjugate anti-hypertensive vaccine. Sci Rep. 2017;7:12580.